INTERPRETATION OF ARTIFICIAL AND ENVIRONMENTAL TRACERS IN FISSURED ROCKS WITH A POROUS MATRIX

P. MAŁOSZEWSKI, A. ZUBER
Institute of Nuclear Physics,
Cracow, Poland

Abstract

INTERPRETATION OF ARTIFICIAL AND ENVIRONMENTAL TRACERS IN FISSURED ROCKS WITH A POROUS MATRIX.

Tracer movement in fissured rocks with a porous matrix is considered. Solutions to the transport equation for the piston-flow and dispersion models in the case of instantaneous tracer injection are given. The great number of non-disposable parameters make a correct interpretation of tracer experiments impossible. However, an ordinary dispersion model yields the mean transit time of tracer ($\bar{t}$), which can be easily related to the mean transit time of water (t_0) if the ratio of the matrix porosity (n_p) to the fissure porosity is known, namely $\bar{t} = (1 + n_p/n_f)t_0$. Unfortunately, strong tailing effects make the interpretation difficult to perform for low values of t_0 (fast flow and/or short distance). In the case of environmental tracers it is suggested that the lumped-parameter approach may be applied in its present form, but to obtain the water age it is necessary to introduce a correction similar to that for artificial tracer experiments. However, this simple correction applies only if $(\lambda/D_p)^{1/2} L/2 \leq 0.25$ (λ is the decay constant, D_p is diffusion in the matrix, L is fissure spacing). In other cases the correction must involve the above-given decay term. Fortunately, this term decreases the correction factor. However, both the fissure spacing (L) and the fissure porosity (n_f) are very difficult to evaluate. Thus, in most cases, a tracer experiment will not yield the required information.

1. INTRODUCTION

The aim of this paper is to describe the influence of molecular diffusion in a porous matrix on the interpretation of tracer experiments in fissured rocks. In 1975, Foster [1] pointed out that the anomalously low tritium contents in the Chalk aquifer in the United Kingdom can be explained by diffusion of tritium into the porous matrix during infiltration through the unsaturated zone. Since then, much attention has been paid to solute transport through fissured media with a porous matrix [2–10]. Most of the publications deal with the movement of contaminants and/or the problems of ^{14}C age determination. An attempt was also made to apply the theoretical plate model developed in gas chromatography to the interpretation of tracer experiments [11, 12]. In the present paper the

attention is focused on the interpretation of artificial tracer experiments as well as on environmental tracers variable in time. The piston-flow and dispersion models for fissures with molecular diffusion in the matrix are considered.

2. PHYSICAL ASSUMPTIONS AND MATHEMATICAL MODEL

A system of identical parallel fissures equally spaced in a porous matrix is considered. The tracer appears at the fissure inlet, having been instantaneously injected into inflowing water, and is transported along the fissures by groundwater flow. The flow rate in fissures is assumed to be fast enough to neglect transport in the axial direction through the porous matrix. The distribution of tracer across the fissure width is assumed to be constant owing to sufficient transverse dispersion and diffusion. Under these assumptions, the following equations for mass balance in fissures and in the matrix can be used:

$$\frac{\partial c_f}{\partial t} + v\frac{\partial c_f}{\partial x} - D\frac{\partial^2 c_f}{\partial x^2} + \lambda c_f - \frac{n_p D_p}{b}\frac{\partial c_p}{\partial y}\bigg|_{y=b} = 0 \tag{1}$$

$$\frac{\partial c_p}{\partial t} - D_p\frac{\partial^2 c_p}{\partial y^2} + \lambda c_p = 0 \quad \text{for } b \leqslant y \leqslant L/2 \tag{2}$$

where c_f and c_p are the tracer concentrations in water in the fissures and in the matrix, respectively, v is the mean water velocity in the fissures, x is the spatial co-ordinate taken in the direction of flow, y is the spatial co-ordinate perpendicular to the fissure extension, t is the time variable, λ in the decay constant, n_p is the matrix porosity, D_p is the molecular diffusion coefficient in the porous matrix, D is the dispersion coefficient in the fissures, 2b is the fissure aperture, and L is the fissure spacing.

Equation (1) describes the convective and dispersive transport in fissures, Eq.(2) the diffusive transport in the matrix in the direction perpendicular to fissures. The following initial and boundary conditions are used to solve these equations for instantaneous injection:

$$c_f(x,0) = 0 \tag{3a}$$

$$c_f(0,t) = A_0\delta(t) \tag{3b}$$

$$c_f(\infty,t) = 0 \tag{3c}$$

$$c_p(y,x,0) = 0 \tag{4a}$$

$$c_p(b,x,t) = c_f(x,t) \tag{4b}$$

$$\frac{\partial c_p}{\partial y}\left(\frac{L}{2}, x, t\right) = 0 \tag{4c}$$

where $A_0 = A/(n_f vS)$, A being the injected mass or the activity, S the cross-section area perpendicular to flow, and n_f the fissure porosity ($n_f = 2b/L$). Solutions to Eqs (1) and (2) for conditions (3) and (4) are given in the Appendix.

3. CONCENTRATION CURVES FOR INSTANTANEOUS INJECTION OF A CONSERVATIVE TRACER

It is shown in the Appendix that, to a good approximation, the mean transit time of a conservative tracer ($\bar{t}$) is related to the mean transit time of water (t_0) by

$$\bar{t} \cong (1 + n_p/n_f)t_0 = R_p t_0 \tag{5}$$

where R_p is the retardation factor given as the ratio of the total porosity to the fissure porosity. Equation (5) means that the flow velocity in fissures is not measurable by the tracer method unless the n_p/n_f ratio is known with sufficient accuracy.

Consider now concentration curves for a piston-flow model ($D = 0$ in Eq.(1)). Examples of such curves, computed from Eq.(A.11) (see Appendix), are shown in Fig.1. Computational difficulties encountered at the time of writing this paper prevented us from obtaining curves for flow times of the order of days. In spite of this, several conclusions can be drawn from Fig.1. For low flow and/or large distances, i.e. for high values of $t_0 = x/v = V_f/Q$ (V_f is the mobile water volume, i.e. the volume of fissures, and Q is the volumetric flow rate through the system), the tracer moves as if it moved homogeneously through the total porosity, because the tracer curves have a tendency to become almost symmetrical around the mean value given by Eq.(5). For fast flow and/or short distance, i.e. for low values of $t_0 = x/v$, the tracer curves are highly asymmetrical. If, in addition, the retardation factor is low ($1 + n_p/n_f < 2$), the time of maximum concentration is close to t_0, and this time may, to a rough approximation, serve for estimating t_0. However, for increasing values of the retardation factor, the tracer curves become more shifted, and the position of c_{max} does not correspond to t_0 even in approximation.

It should be noted that there are six (five) departure parameters in the dispersion model (piston-flow model). These parameters are: v (or t_0 for a given x), L (or n_f), n_p (or R_p), b, D_p and D (or $D/v = \alpha_L$, or $D/(vx) = Pe^{-1}$). These parameters can be reduced to four or three non-disposable parameters by putting

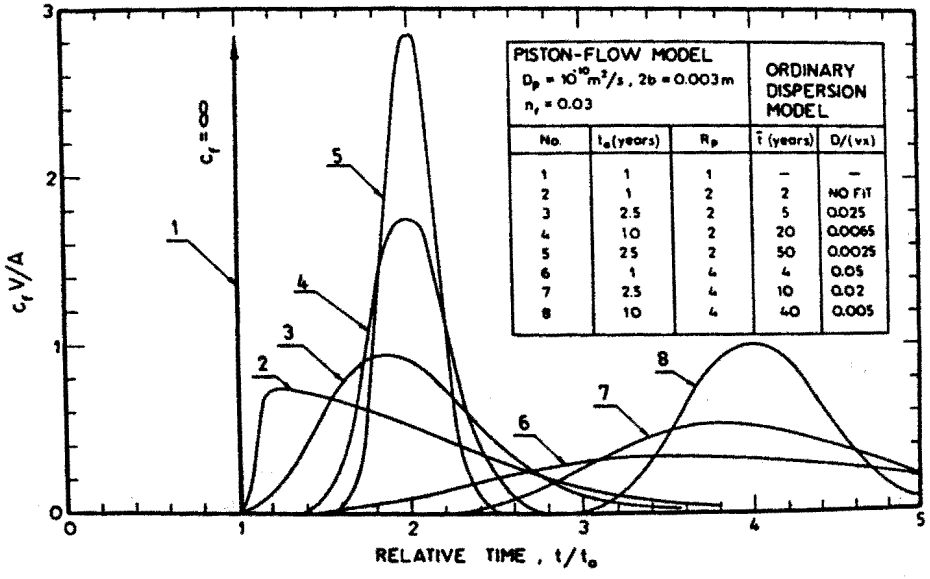

FIG.1. Examples of concentration curves for the piston-flow model with diffusion, and for the ordinary dispersion model with $\bar{t} = (1 + n_p/n_f)t_0$.

$a = n_p(D_p)^{1/2}/(2b)$ and $\delta = (L/2 - b)(D_p)^{-1/2}$. Then there are four parameters $(D/(vx), t_0, a, \delta)$ for the dispersion model and three (t_0, a, δ) for the piston-flow model. The retardation factor can be given as $R_p = 1 + 2a\delta$. A high number of non-disposable (fitting) parameters make the solution to the inverse problem (calibration of the model) rather questionable. It is thus of interest to investigate whether simpler models can supply any information when fitted to the experimental tracer curves.

Here this problem is investigated by comparing the theoretical tracer curves of simple models with those of models more adequately corresponding to the physical situation. In Fig.1, curves 3 to 8 also represent, within the accuracy of the drawn lines, the ordinary dispersion model, introduced in hydrology in Ref.[13] and described in detail in Ref.[14]. This model in the non-normalized form reads

$$c(x,t) = \frac{A\,x}{nSv\sqrt{(4\pi Dt^3)}} \exp\left[-\frac{(x-vt)^2}{4Dt}\right] \qquad (6)$$

Other ordinary dispersion models can also be used in the cases of low dispersion, as discussed in Ref.[14]. However, it appears that in order to fit the model (6) to the concentration curves of the model (A.11), the mean water velocity (v) has

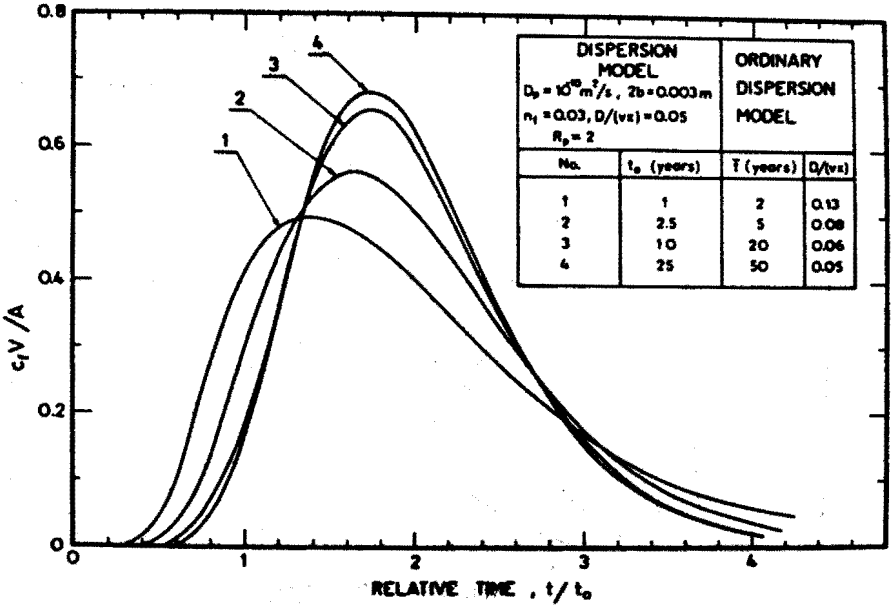

FIG.2. Examples of concentration curves for the dispersion model with diffusion, and for the ordinary dispersion model with $\bar{t} = (1 + n_p/n_f)t_o$.

to be replaced by the mean tracer velocity, which is obtainable directly from Eq.(5), namely $\bar{v}_{tracer} = v/R_p$. If Eq.(6) is normalized to obtain dimensionless concentration and time and to reduce the space variable, the following form is obtained after introducing Eq.(5):

$$\frac{c_f V}{A} = \frac{\sqrt{Pe}}{\sqrt{[4\pi(t/\bar{t})^3]}} \exp\left[-\frac{(1-t/\bar{t})^2}{4Pe^{-1}\, t/\bar{t}}\right] \qquad (7)$$

where V is the total volume occupied by water ($V = R_p V_f$), and $Pe^{-1} = D/(\bar{v}_t x)$ is an apparent dispersion parameter in which the velocity is transferred, using the retardation factor, with D an apparent dispersion coefficient involving also the dispersion caused by diffusion into the matrix (D/v is the longitudinal dispersivity, commonly denoted as α_L). In Figs 1–3, Eq.(7) is used as the ordinary dispersion model. It is clear from Fig.1 that the ordinary dispersion model gives the same concentration curves as model (A.11), except for fast flow (low t_o value) and low values of R_p. The same conclusions can be drawn from Figs 2 and 3, where dispersion in the fissures is taken into account (Eq.(A.10)). However, it may be suspected that in cases of high dispersion in fissures, fast flow and low values of $R_p = (n_f + n_p)/n_f$, the maximum concentration may appear even at times shorter

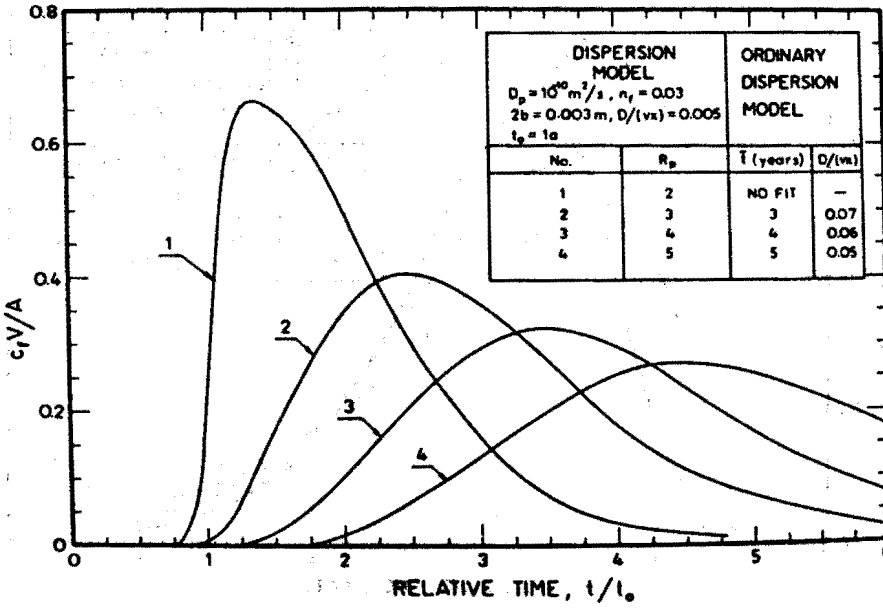

FIG.3. Examples of concentration curves for the dispersion model with diffusion, and for the ordinary dispersion model with $\bar{T} = (1 + n_p/n_f)t_0$. *(Parameters are different from those of Fig.2.)*

than t_0. This suspicion is based on the inspection of concentration curves representing Eq.(6) (see, for instance, Ref.[13]). Computational difficulties connected with oscillations of Eqs (A.10) and (A.11) prevented us from clarifying this problem.

It should be noted that Eqs (6), (A.10) and (A.11) as well as Eq.(11) were derived for semi-infinite media. However, assuming that the second boundary (end of a finite system) does not influence the hydrodynamic dispersion in the system, they are also applicable to finite systems.

4. EXPERIMENTAL VERIFICATION

The laboratory experiment of Grisak et al. [3, 4], performed with a fractured clay-loam till, is used here for verifying some ideas presented in the previous section. A till sample, 0.76 m long and 0.65 m in diameter, was placed in a cylindrical drum. Two sets of orthogonal fractures were oriented vertically in the column parallel to the long axis and to the flow direction. The fracture spacing was not well known. According to Ref.[3], an experiment with air bubbles yielded 10 cm spacing in both directions. However, fitting of the tracer curve yielded a

6 cm spacing [3], whereas in Ref.[4] a 4 cm spacing was reported. For a given spacing (L), the fracture aperture (2b) and flow velocity (v) became disposable in that experiment because [3]

$$(2b)^3 = \frac{Q}{S} \frac{12\mu}{\rho g(dh/dx)} L \tag{8}$$

$$v = Sn_f/Q = 2(2b)S/(LQ) \tag{9}$$

where Q is the volumetric flow rate through the sample, S is the total cross-sectional area of the sample, μ is the dynamic viscosity, ρ is the fluid density, g is the gravitational acceleration, and dh/dx is the hydraulic gradient. An additional factor of 2 results from the presence of two sets of fissures.

The following parameters were applied in Ref.[3] and are also used here: L = 6 cm, 2b = 40 μm, v = 29.7 m·d^{-1} and n_p = 0.35. From these data, the retardation factor is

$$R_p = 1 + n_p/n_f = 1 + Ln_p/(4b) = 1 + 0.35 \times 6/(80 \times 10^{-6}) = 264 \tag{10}$$

and the mean velocity of the tracer is $\bar{v}_t = v/R_p = 29.7\ m \cdot d^{-1}/264 = 0.112\ m \cdot d^{-1}$. In Fig.4, the experimental points represent the passage of chloride anions continuously injected; curve 6 represents the results of a simulation of a numerical solution to Eqs (1) and (2) [3]. The other curves represent the ordinary dispersion model. Because of continuous injection, instead of Eq.(6) its integrated form must be used [14]. This well-known solution reads:

$$c_f/c_0 = \frac{1}{2}\text{erfc}\left[\frac{x-vt}{\sqrt{(4Dt)}}\right] + \frac{1}{2}\exp\left(\frac{xv}{D}\right)\text{erfc}\left[\frac{x+vt}{\sqrt{(4Dt)}}\right] \tag{11}$$

This equation fits the discussed laboratory data if the velocity is adequately transferred ($\bar{v}_t$ = 0.112 m·d^{-1}) and an apparent high dispersivity is selected. It may be worth mentioning that, without knowledge of Eq.(5), Grisak et al. [3] came to the conclusion that no fit of Eq.(11) is possible (see Fig.4, curve 1, for real v, and curve 2 for arbitrary $\bar{v}_t$ and a reasonable α_L value). Curve 5 shows the concentration that would be observed if an instantaneous injection were performed. From the shape of this curve, showing a very long tail, it may be concluded that the mean tracer transit time cannot be determined with good accuracy (see Appendix for the definition of $\bar{t}$ and imagine the length of the tail of curve 5 in Fig.4 for $\bar{t} = x/\bar{v}_t$ = 0.76 m/0.122 d = 6.8 days). The problem of the interplay of parameters in the dispersion model was quantitatively studied by Kreft [15]. We illustrate this problem by an example: Curve 3 in Fig.4, calculated for arbitrary $\bar{v}_t$, gives an equally good fit as curve 4 for which $\bar{v}_t$ is calculated with the

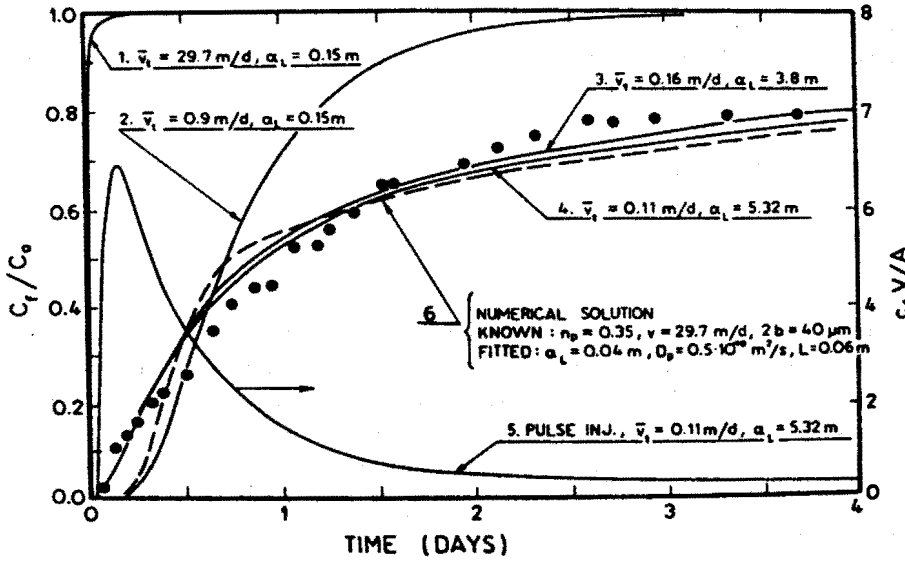

FIG.4. Experimental data and theoretical curves for continuous tracer injection. Curves 1 to 4 – ordinary dispersion model for different $\bar{t}$ (4 – for $\bar{t} = R_p t_0$); curve 5 would correspond to curve 4 if the tracer were injected instantaneously; curve 6 – simulated for a numerical solution to Eqs (1) and (2). The experimental data and curves 1, 2 and 6 are from Ref.[3].

aid of Eq.(5). This means that in the case of a high apparent dispersion no exact determination of parameters is possible.

5. DISCUSSION OF TRACER EXPERIMENTS IN FISSURED ROCKS

Space limitation and the preliminary stage of this study do not permit of a detailed discussion of the known tracer experiments in fissured rocks. Undoubtedly, all these experiments should be reinterpreted. For instance, the two-well method invented for measuring the effective (mobile water) porosity in fact yields the total accessible porosity following from Eq.(5).

In the case of a low matrix porosity with respect to the fissure porosity (low values of R_p), a tracer experiment yields approximate flow parameters (e.g. groundwater velocity). In other cases, a tracer experiment is little related to flow parameters and its interpretation in terms of flow parameters is highly questionable.

In the case of a high apparent dispersion, in addition to the interplay of parameters discussed in Section 4, there are practical problems related to the measurement of the tail part of the concentration curve. Most probably, in many field experiments this part was not measurable and in consequence the mean transit time obtained from these experiments represented neither the flow in

fissures nor the apparent flow through the total porosity. Note that a high dispersion may result either from the discussed diffusion effects (then it is an apparent dispersion) or from a wide distribution of the fissure width, as shown in Ref.[7]. Of course, in the case of a high real dispersion the peak concentration does not correspond to the water velocity [13]. In other words, if there is no additional information on the investigated system, the interpreter will not know which model to use.

6. INTERPRETATION OF ENVIRONMENTAL RADIOISOTOPE TRACERS IN A STEADY STATE

Applying the piston-flow model, which for a steady input concentration is a very good approximation in systems with a distant recharge (low values of the apparent dispersion parameter), the radioisotope (e.g. ^{14}C) age of water is defined from

$$c_f/c_0 = \exp(-\lambda t_a) \tag{12}$$

Combining Eq.(12) with the solution to Eqs (1) and (2) for a steady state, we obtain

$$t_a/t_0 = 1 + n_p \,\mathrm{tgh}(p)/(n_f p) \tag{13}$$

where $p = (\lambda/D_p)^{1/2} \cdot (L/2 - b)$. For $p \leqslant 0.25$,

$$t_a/t_0 = 1 + n_p/n_f = R_p \tag{14}$$

whereas for $p \geqslant 2$,

$$t_a/t_0 = 1 + n_p/(n_f p) \tag{15}$$

however for $L \to \infty$ (i.e. for a single fissure), $n_p/n_f \to \infty$ and $p \to \infty$, and then

$$t_a/t_0 = 1 + (n_p/b)\sqrt{(D_p/\lambda)} \tag{16}$$

Equation (13) is equivalent to Eq.(7) of Ref.[6], but the form given here is simpler. Equation (16) is equivalent to Eq.(B.5) of Ref.[5]. A graphical presentation of Eq.(13) is given in Fig.5.

It is worth mentioning that if in Eq.(2), b is replaced by the half-thickness of an aquifer (h/2) times aquifer porosity (n), and if n_p is replaced by the aquitard porosity (n_a), we obtain

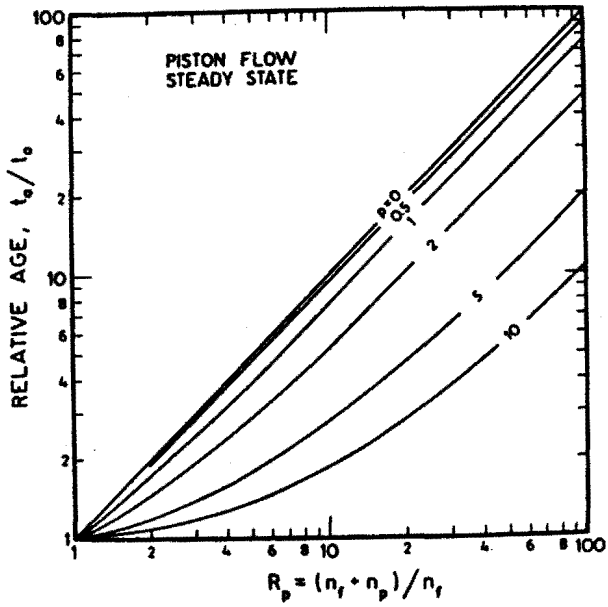

FIG.5. Relative radioisotope age determined from the piston-flow model for steady-state input (Eq.(13)).

$$t_a/t_0 = 1 + [2n_a/(hn)]\sqrt{(D_a/\lambda)} \qquad (17)$$

where t_a is the radioisotope age (Eq.(12)) in a layered aquifer with a two-side diffusion into porous aquitards, and D_a is the diffusion coefficient in the aquitard. Equation (17) gives practically the same values of t_a/t_0 as the more sophisticated Eq.(13) in Ref.[16], which was obtained by taking into account the aquifer dispersivity. If a porous aquitard is on one side of the aquifer, the factor 2 disappears in Eq.(16).

7. INTERPRETATION OF ENVIRONMENTAL TRACERS VARIABLE IN TIME

One commonly applied environmental tracer is variable in time, namely tritium, and several other potential tracers, such as ^{85}Kr, freons and tritiugenic ^{3}He, are also variable in time [17, 18]. Usually, the so-called lumped-parameter models are used in the convolution integral which relates the input (c_{in}) and output (c) concentrations

$$c(t) = \int_0^\infty c_{in}(t-t')\exp(-\lambda t')g(t')dt' \qquad (18)$$

where g(t) is the weighting function, also called the exit age distribution of tracer particles which entered the system at a given time t = 0 [18, 19]. Groundwater systems, contrary to laboratory arrangements and industrial systems, have their entrances (recharge areas) extended in space and thus the physical meaning of the parameters of the weighting function is somewhat different from what it is in a strictly unidimensional case for which Eq.(18) was developed. For instance, if the dispersion model is used for g(t), then the dispersion parameter is an apparent quantity which practically has no relation to the dispersivity of the system but depends on the relation between the extent of the recharge area and the distance to the measuring point [17, 18]. Thus, it would be quite unrealistic to put as g(t) the solutions to Eqs (1) and (2), which involve the microscopic phenomena and their relations to the mean velocity and dispersivity in a system of identical fissures. It seems that an exact solution of the problem is not possible at all. To obtain some estimate, consider first the mean transit time of a decaying tracer. Applying the procedure described in the Appendix, the following formula is obtained for the piston-flow model:

$$\bar{t}/t_0 = 1 + \frac{n_p(L-2b)}{2b}\left|\frac{\mathrm{tgh}(p)}{2p} + \frac{1}{2}\cosh^{-2}(p)\right| \qquad (19)$$

For $L \gg 2b$ and $p \leqslant 0.25$, Eq.(19) simplifies to

$$\bar{t}/t_0 = 1 + n_p/n_f \qquad (20)$$

whereas, for $p \geqslant 3$,

$$\bar{t}/t_0 = 1 + (n_p/n_f)/(2p) \qquad (21)$$

Figure 6 shows graphs of $\bar{t}/t_0$. In approximation, it may be assumed that the tracer in each flow line is delayed according to Eq.(19). Thus the apparent age, interpreted with the aid of an ordinary lumped-parameter model as applied in Eq.(18), has to be corrected as follows:

$$t_0(\text{true}) = t_0(\text{apparent})/(\bar{t}/t_0) \qquad (22)$$

where $\bar{t}/t_0$ is determined from Fig.6 or directly from Eq.(19). At a first glance, the situation seems to be hopeless because a great number of parameters have to

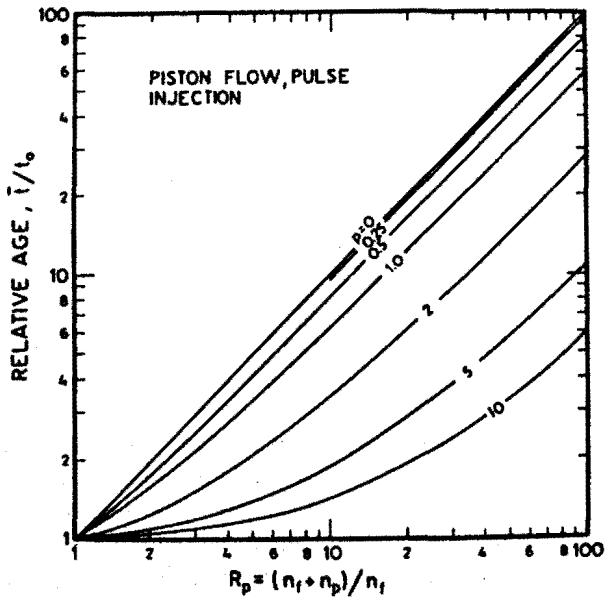

FIG.6. Relative mean transit time of a radioisotope for the piston-flow model (Eq.(19)), representing in approximation the relative age as determined by ordinary lumped-parameter models for variable inputs (Eq.(18)).

be known. However, it appears that in many cases the simplified form given by Eq.(20) applies, i.e. for ^{14}C ($\lambda = 3.83 \times 10^{-12}$ s^{-1}) and $D_p = 0.5 \times 10^{-10}$ m$^2 \cdot$s^{-1} (value found for fractured till in Ref.[3] – see also Fig.4), p is below 0.25 if $L < 1.8$ m. Then

$$t_o(\text{true}) = t_o\ (\text{apparent})/(1 + n_p/n_f) \tag{23}$$

which requires only an estimate of n_p/n_f. In the case of tritium ($\lambda = 18 \times 10^{-10}$ s^{-1}), Eq.(23) applies if $L < 0.083$ m for the same D_p as above. In other cases the difference between the true and apparent values will be lower than that indicated by Eq.(23), as can be seen from Fig.6.

Similar conclusions can be drawn from the dispersion model, for which

$$\bar{t}/t_o = \text{Eq.(19)} \Bigg/ \left| 1 + 4Pe^{-1} t_o \lambda \left| 1 + \frac{n_p(L-2b)\,\text{tgh}(p)}{2\,bp} \right| \right|^{1/2} \tag{24}$$

Equation (24) shows that the dispersivity in fissures decreases the retardation, which is in agreement with earlier findings [20]. However, judging from the

experiment described in Section 4, the microdispersivity in fissures is rather low, of the order of centimetres. This means that for experimental situations involving environmental radioisotope problems the dispersion term in Eq.(24) is usually negligible. On the other hand, a high dispersivity in a fissured medium may be observed if the fissure widths are highly distributed [7]. If the fissure widths remain constant along the entire system length, the dispersivity will be proportional to the distance. However, in most groundwater systems, the fissures are of limited length and consequently the dispersivity becomes constant and is usually not greater than a few metres. Thus the dispersion parameter $(D/(vx) = \alpha_L/x)$ becomes very low for large distances and consequently the piston-flow approximation (Eq.(19)) may probably be used instead of Eq.(24).

8. CONCLUSIONS

Solute transport in fissured rocks with a porous matrix is described by multi-parameter models. Thus an unambiguous interpretation of tracer experiments is not possible with the aid of these models. The ordinary dispersion model, applied to long-term experiments, yields an apparent transit time related to total porosity. In short-term experiments, the determination of the mean transit time of tracer is ambiguous because of a high apparent dispersivity and strong tailing effects.

Environmental tracers interpreted with the aid of ordinary lumped-parameter models yield apparent ages greater than the real ages. Under favourable conditions the real age can be found if the ratio of matrix porosity to fissure porosity is known.

The development of mathematical models describing solute movement in fissured media with a porous matrix is the main theoretical achievement of recent years. However, the interpretation of tracer experiments requires further studies.

Appendix

Equations (1) and (2) with initial and boundary conditions (3) and (4) can be solved by applying the Laplace transform, similarly to the solution presented in Ref.[9] for continuous injection. In this way, instead of Eqs (1) and (2), one obtains ordinary differential equations

$$(p+\lambda)\bar{c}_f + v\frac{d\bar{c}_f}{dx} - D\frac{d^2\bar{c}_f}{dx^2} - \frac{n_p D_p}{b}\frac{d\bar{c}_p}{dy}\bigg|_{y=b} = 0 \qquad \text{(A.1a)}$$

$$(p+\lambda)\,\bar{c}_p - D_p \frac{d^2\bar{c}_p}{dy^2} = 0 \tag{A.1b}$$

where

$$\bar{c}_f = \int_0^\infty e^{-pt} c_f(x,t)\,dt \qquad \bar{c}_p = \int_0^\infty e^{-pt} c_p(y,x,t)\,dt$$

The general solution of Eq.(A.1b) is

$$\bar{c}_p = A_1 \exp(r_1 y) + A_2 \exp(r_2 y)$$

where $r_{1,2}$ are the square roots of $p + \lambda - r^2 D_p = 0$, i.e. $r_{1,2} = \pm[(p+\lambda)/D_p]^{1/2}$. The constants A_1 and A_2 are found by applying conditions (4), which lead to

$$\bar{c}_p = \bar{c}_f \frac{\cosh\{[(p+\lambda)/D_p]^{1/2}(L/2-y)\}}{\cosh\{[(p+\lambda)/D_p]^{1/2}(L/2-b)\}} \tag{A.2}$$

By finding $\left.\frac{d\bar{c}_p}{d_y}\right|_{y=b}$ and introducing it to (A.1a), one obtains

$$\frac{d^2\bar{c}_f}{dx^2} - \frac{v}{D}\frac{d\bar{c}_f}{dx} - \frac{\bar{c}_f}{D}\left\{(p+\lambda) + \frac{n_p\sqrt{D_p}}{b}\cdot\sqrt{(p+\lambda)}\right.$$
$$\left.\times \operatorname{tgh}\left[\frac{L/2-b}{\sqrt{D_p}}\sqrt{(p+\lambda)}\right]\right\} = 0 \tag{A.3}$$

The general solution of Eq.(A.3) is similar to the general solution of Eq.(A.1b), where $r_{1,2}$ are the square roots of

$$r^2 - \frac{v}{D}r - \frac{1}{D}\left\{(p+\lambda) + \frac{n_p\sqrt{D_p}}{b}\sqrt{(p+\lambda)}\operatorname{tgh}\left[\frac{L/2-b}{\sqrt{D_p}}\sqrt{(p+\lambda)}\right]\right\} = 0$$

By applying conditions (3) for the determination of constants A_1 and A_2, one obtains

$$\bar{c}_f = A_0 \exp\left\{\frac{vx}{2D}\left[1 - \left\{1 + \frac{4D}{vx}t_0[(p+\lambda) + (n_p/b)\sqrt{D_p(p+\lambda)}\right.\right.\right.$$
$$\left.\left.\left.\times \operatorname{tgh}((L/2-b)\sqrt{(p+\lambda)}/\sqrt{D_p})]\right\}^{1/2}\right]\right\} \tag{A.4}$$

where $t_0 = x/v$.

Equation (A.4) is the Laplace transform of the sought tracer distribution in fissures. From this equation the mean transit time of tracer can be found without finding the inverse transform. The mean tracer transit time is defined as

$$\bar{t}(x) = \int_0^\infty t c_f(x,t)dt \Big/ \int_0^\infty c_f(x,t)dt \qquad (A.5)$$

which can be transformed to

$$\bar{t} = \lim_{p \to 0} \left(-\frac{d\bar{c}_f}{dp}\right) \Big/ \lim_{p \to 0} \bar{c}_f \qquad (A.6)$$

By inserting Eq.(A.4) into Eq.(A.6), one obtains for a conservative tracer (i.e. for $\lambda = 0$ in the case of a non-adsorbable substance):

$$\bar{t} = t_0 [1 + n_p(L-2b)/2b] \cong t_0 \, (1 + n_p/n_f) \qquad (A.7)$$

where $n_f = 2b/L$ is the fissure porosity. The same formula is obtainable for the piston-flow model, i.e. when $D = 0$ in Eq.(1).

The concentration distribution in the fissures can be calculated from Eq.(A.4) by simplifying it with the aid of the following expressions

$$\exp(-2\Theta) = \frac{2}{\sqrt{\pi}} \int_0^\infty \exp[-\xi^2 - (\Theta/\xi)^2]d\xi$$

where

$$\Theta = \tfrac{1}{2}\gamma \{1 + \beta^2 [p + \sqrt{p}\,\kappa^{-1} \operatorname{tgh}(\delta\sqrt{p})]\}^{1/2}$$

$$\gamma = \frac{vx}{2D}, \quad \beta^2 = 4\frac{D}{vx} t_0, \quad \kappa^{-1} = \frac{n_p\sqrt{D_p}}{b} \quad \text{and}$$

$$\delta = (L/2 - b)/\sqrt{D_p}$$

After substitutions and rearrangements, Eq.(A.4) takes the form

$$\frac{\tilde{c}_f}{A_0} = \frac{2}{\sqrt{\pi}} \exp(\gamma) \int_0^\infty \exp\left(-\xi^2 - \frac{\gamma^2}{4\xi^2}\right) \cdot \exp[-F(\xi\sqrt{p}\,\mathrm{tgh}(\delta\sqrt{p})]$$

$$\times \exp[-\kappa F(\xi) p] d\xi \tag{A.8}$$

where $F(\xi) = (\gamma\beta)^2/(4\xi^2\kappa)$.

Knowing that

$$L^{-1}\{\exp[-Y\sqrt{p}\,\mathrm{tgh}(Z\sqrt{p})]\} = \frac{1}{\pi} \int_0^\infty \epsilon \exp(\epsilon_R) \cos(\epsilon_I) d\epsilon \tag{A.9}$$

where

$$\epsilon_R = -\frac{Y\epsilon}{2} \frac{\sinh(Z\epsilon) - \sin(Z\epsilon)}{\cosh(Z\epsilon) + \cos(Z\epsilon)}$$

$$\epsilon_I = \frac{\epsilon^2 t}{2} - \frac{Y\epsilon}{2} \frac{\sinh(Z\epsilon) + \sin(Z\epsilon)}{\cosh(Z\epsilon) + \cos(Z\epsilon)}$$

one finally obtains

$$\frac{c_f(x,t)}{A_0} = \frac{2}{\pi^{3/2}} \exp\left(\frac{vx}{2D}\right) \int_w^\infty \exp\left[-\xi^2 - \left(\frac{vx}{4D\xi}\right)^2\right]$$

$$\times \left[\int_0^\infty \epsilon \exp(-\epsilon_1) \cos(\epsilon_2) d\epsilon\right] d\xi \tag{A.10}$$

where

$$w = \frac{1}{2}\left(\frac{vx}{D}\frac{t_0}{t}\right)^{1/2}$$

$$\epsilon_1 = \frac{vx}{8D} t_0 \frac{n_p\sqrt{D_p}}{b} \frac{\epsilon}{\xi^2} \frac{\sinh(\delta\epsilon) - \sin(\delta\epsilon)}{\cosh(\delta\epsilon) + \cos(\delta\epsilon)}$$

$$\epsilon_2 = \frac{\epsilon^2}{2}\left(t - \frac{vx}{4D}\frac{t_0}{\xi^2}\right) - \frac{vx}{8D} t_0 \frac{n_p\sqrt{D_p}}{b} \frac{\epsilon}{\xi^2} \times \frac{\sinh(\delta\epsilon) + \sin(\delta\epsilon)}{\cosh(\delta\epsilon) + \cos(\delta\epsilon)}$$

In the case of the piston-flow model, i.e. for D = 0 in Eq.(1), the solution reads

$$\frac{c_f(x,t)}{A_0} = \frac{1}{\pi}\int_0^\infty \epsilon \exp(-\epsilon_3)\cos(\epsilon_4)d\epsilon \text{ for } t \geqslant t_0 \qquad (A.11)$$

where

$$\epsilon_3 = \frac{n_p\sqrt{D_p}}{2b}\, t_0\epsilon \frac{\sinh(\delta\epsilon)-\sin(\delta\epsilon)}{\cosh(\delta\epsilon)+\cos(\delta\epsilon)}$$

$$\epsilon_4 = (t-t_0)\frac{\epsilon^2}{2} - \frac{n_p\sqrt{D_p}}{2b}\, t_0\epsilon \frac{\sinh(\delta\epsilon)+\sin(\delta\epsilon)}{\cosh(\delta\epsilon)+\cos(\delta\epsilon)}$$

REFERENCES

[1] FOSTER, S.S.D., J. Hydrol. 25 (1975) 159.
[2] GRISAK, G.E., PICKENS, J.F., Water Resour. Res. 16 4 (1980) 719.
[3] GRISAK, G.E., PICKENS, J.F., CHERRY, J.E., Water Resour. Res. 16 4 (1980) 731.
[4] GRISAK, G.E., PICKENS, J.F., J. Hydrol. 52 (1981) 47.
[5] NERETNIEKS, I., J. Geophys. Res. 85 B8 (1980) 4379.
[6] NERETNIEKS, I., Water Resour. Res. 17 2 (1981) 421.
[7] NERETNIEKS, I., ERIKSEN, T., TAHTINEN, P., Water Resour. Res. 18 4 (1982) 849.
[8] TANG, D.H., FRIND, E.O., SUDICKY, E.A., Water Resour. Res. 17 3 (1981) 555.
[9] SUDICKY, E.A., FRIND, E.O., Water Resour. Res. 18 6 (1982) 1634.
[10] FREEZE, J.A., CHERRY, J.F., Groundwater, Prentice Hall, Englewood Cliffs, NJ (1979).
[11] GLUECKAUF, E., UKAEA Atomic Energy Research Establishment, Harwell, Rep. AERE-R-9823 (1980).
[12] GLUECKAUF, E., UKAEA Atomic Energy Research Establishment, Harwell, Rep. AERE-R-10043 (1981).
[13] LENDA, A., ZUBER, A., Isotope Hydrology 1970 (Proc. Symp. Vienna, 1970), IAEA, Vienna (1970) 619.
[14] KREFT, A., ZUBER, A., Chem. Eng. Sci. 33 (1978) 1471.
[15] KREFT, A., Problems of mathematical modelling of the hydrodynamic dispersion (in Polish), Proc. Acad. Min. Metall. No. 958, Ser. Math.-Phys.-Chem. No. 61 (1983).
[16] SUDICKY, E.A., FRIND, E.O., Water Resour. Res. 17 4 (1981) 1060.
[17] GRABCZAK, J., ZUBER, A., MAŁOSZEWSKI, P., RÓŻAŃSKI, K., WEISS, W., ŚLIWKA, I., Beiträge zur Geologie der Schweiz, Hydrologie 28 II (1982) 395.
[18] ZUBER, A., "Mathematical models for the interpretation of environmental radioisotopes in groundwater systems", Handbook of Environmental Isotope Geochemistry (FRITZ, P., FONTES, J.C., Eds) Vol. 1B, Elsevier, Amsterdam.
[19] MAŁOSZEWSKI, P., ZUBER, A., J. Hydrol. 57 (1982) 207.
[20] RASMUSON, A., NERETNIEKS, I., J. Geophys. Res. 86 B5 (1980) 3749.